

MODELING OF HYDROGEN REDUCTION OF IRON ORE FINES

Henrik Saxén, Emiliano Salucci, Antonio D'Angelo, Henrik Grénman
Åbo Akademi University, Finland

International Conference on
GREEN & SUSTAINABLE IRON MAKING

January 17 – 18, 2024



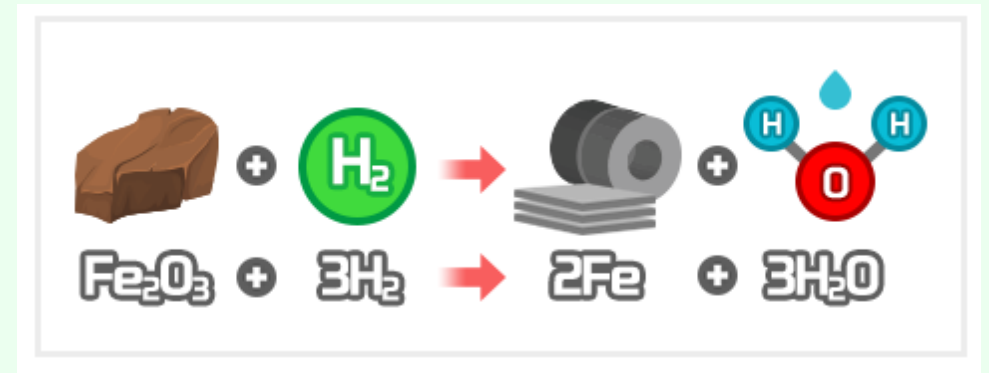
Background

The coal-based steelmaking production (BF-BOF) route is burdened by large CO₂ emissions.

These emissions cannot be dramatically decreased without carbon capture since the BF requires coke to operate properly.

Direct reduction processes reduce iron oxides to metallic iron in solid state using CO and H₂ as reductants.

A new ironmaking route mainly involving a direct reduction furnace operated with pure hydrogen (H₂) is starting to gain worldwide acceptance as an alternative to eliminate the CO₂ emissions in steelmaking.



Main motivation of the work

The kinetics of iron oxide reduction is influenced by several parameters including:

- | | |
|--|--|
| Process parameters: | Properties of the material: |
| <ul style="list-style-type: none"> • Temperature • Pressure • Gas composition | <ul style="list-style-type: none"> • Grain size • Morphology • Impurities • Porosity |

Furthermore, experimental setup, mechanism assumptions and modeling approach must be taken into account.

A wide range of activation energy values has been reported in the literature.

References	Parameter	Activation Energy [kJ mol ⁻¹]
[8]*	Nonisothermal	139.2
[8]**	Nonisothermal	77.3
[8]***	Nonisothermal	85.7
[9]	Powder	47.2
[9]	Powder	51.5
[10]*	Powder	57.1
[10]**	Powder	72.7
[10]***	Powder	89.9
[11]	Pellets	109.9
[11]	Pellets	18
[12]	Pellets	30.1
[13]	Raw material	56.8
[13]	Raw material	72.3
[13]	Raw material	89.4
[14]	Raw material	246
[14]	Raw material	93
[14]	Raw material	162
[14]	Raw material	104
[10]	Impurities	109.9
[10]	Impurities	107.8
[10]	Impurities	129.2
[6]*	Gas Composition	124
[15]*	Gas Composition	139.2
[11]*	Gas Composition	246
[14]*	Gas Composition	162
[16]*	Gas Composition	106
[17]*	Gas Composition	89.1

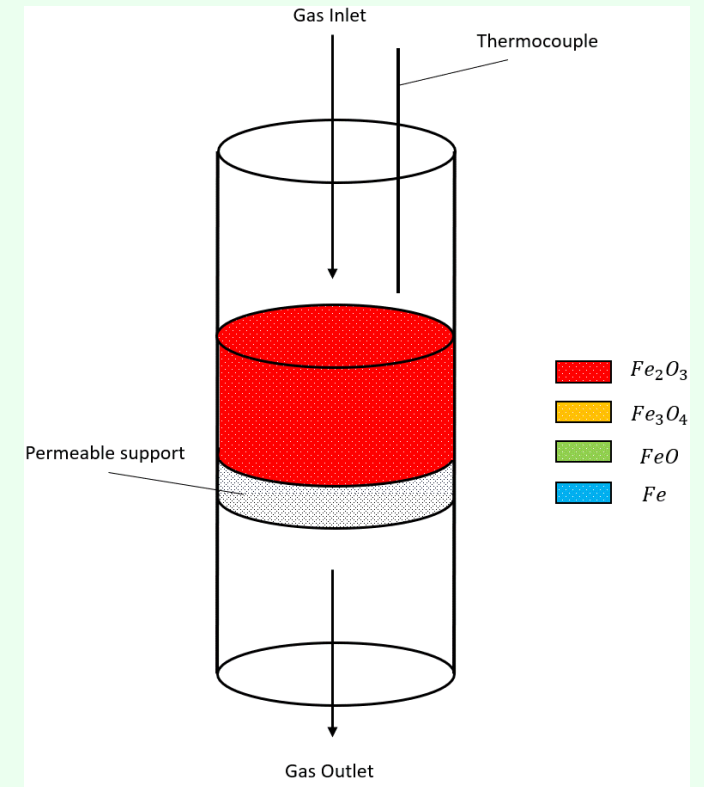
* Hematite-Magnetite reaction; ** Magnetite-Wustite reaction; *** Wustite-Iron reaction

Aim of the work

This work focuses on creation of a mathematical model capable of accurately describing the reduction of iron ores/oxides for developing hydrogen-based DRI processes.

Accurate descriptions of the chemical kinetics and the mass transfer phenomena are crucial for determining the rate-limiting steps and for process simulation.

The final goal is to use the model to estimate kinetic parameters by reverse engineering based on detailed experimental data obtained using a chemisorption device.



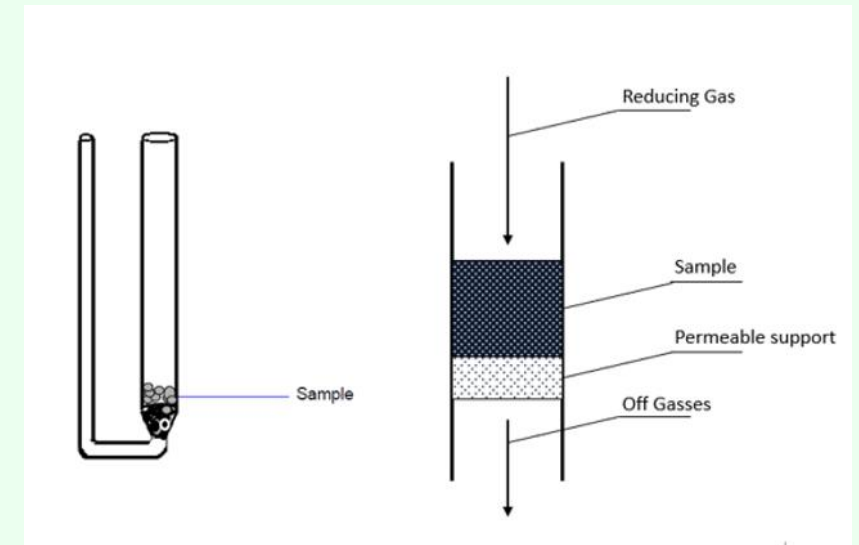
Experimental setup

Reduction test were conducted in a device primarily used for catalyst characterization (chemisorption) consisting of small bed of iron ore/oxides fines, through which the reducing gas passes.

Tests can be conducted varying several operating parameters:

- Temperature
- Reducing gas composition
- Total gas flow rate
- Bed mass

The composition of the gas leaving the bed is analyzed with a thermal conductivity detector (TCD), a mass spectrometer (MS) and gas chromatograph (GC).

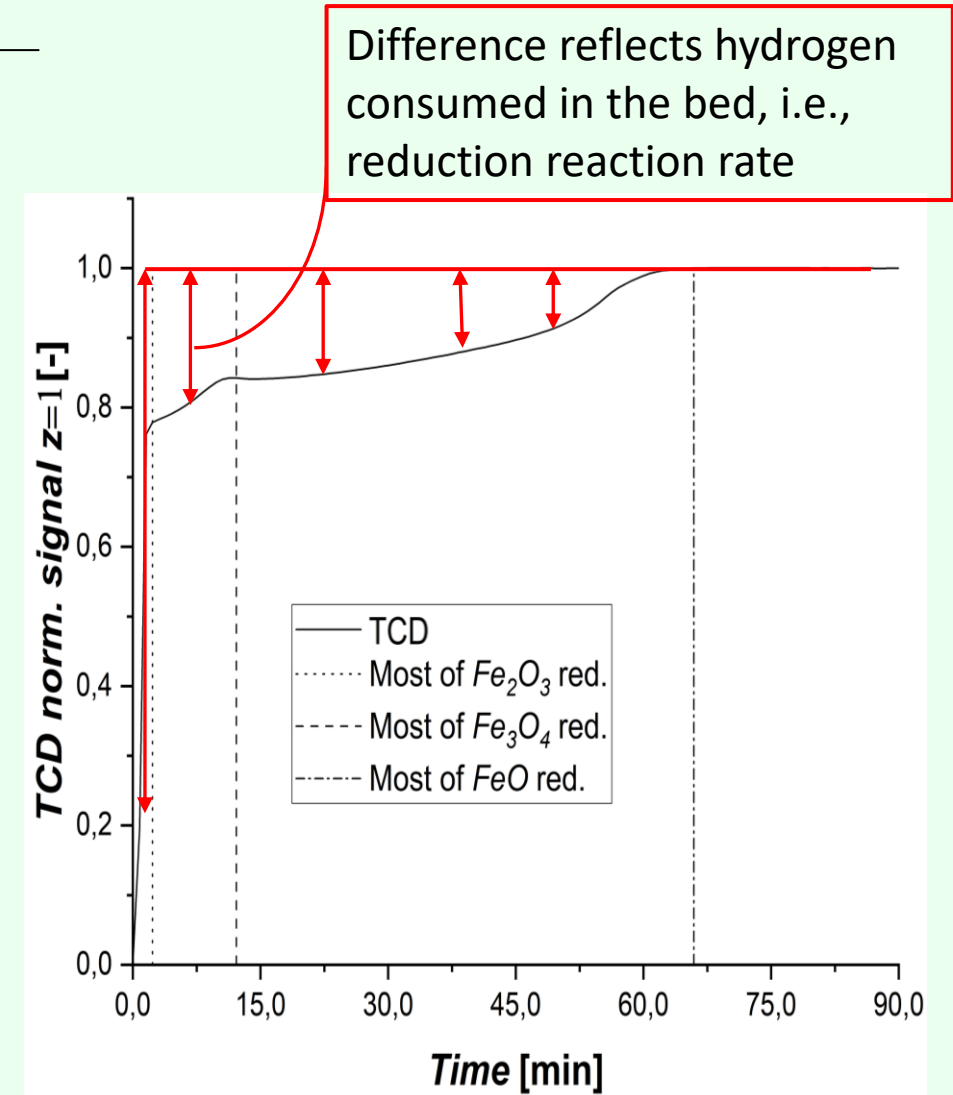


Experiments

Experiments were performed by reducing a bed of fine (micrometer range) iron oxide particles by a gas mixture of H_2 and Ar at different temperatures ranging from 673 K to 1273 K at a total gas flow rate of 8-40 ml/min.

The TCD signal of the off-gas, which largely reflects the hydrogen content of the gas, provides information about the progress of the reduction reactions. If normalized by the thermal conductivity of the entering gas, the reduction has stopped when the value reaches unity.

Different slopes of the curve reflect the progress of the different stages of the reduction, but is somewhat difficult to interpret due to different conditions in the (upper and lower) parts of the bed.

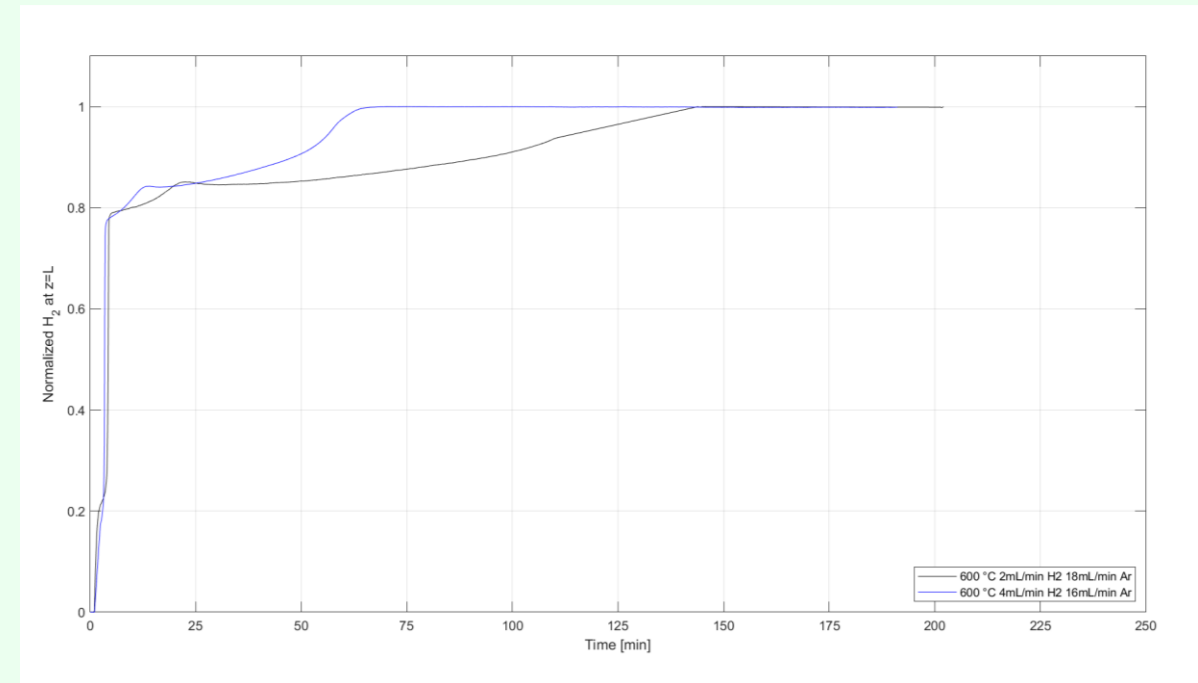
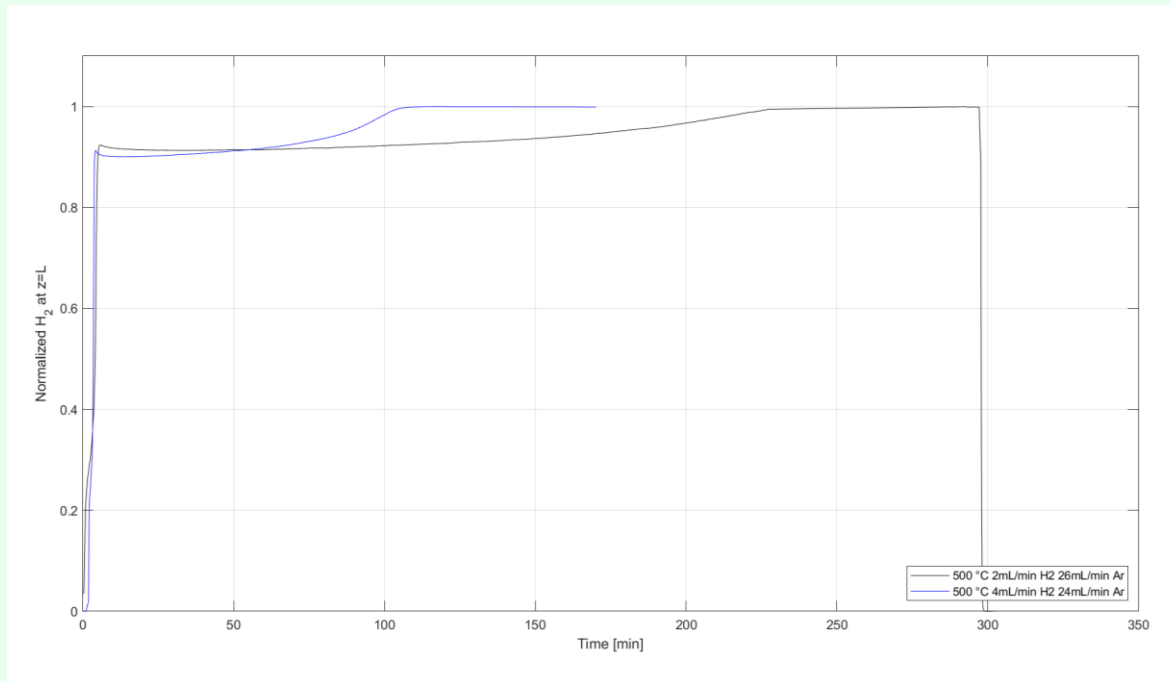


Experimental results: Examples (1)

Normalized TCD results of reduction experiments with a 100 mg bed.

Left panel: 773 K, 7.7 % H₂ (black curve) and 16.7 % H₂ (blue curve). Time to full reduction 110/220 min

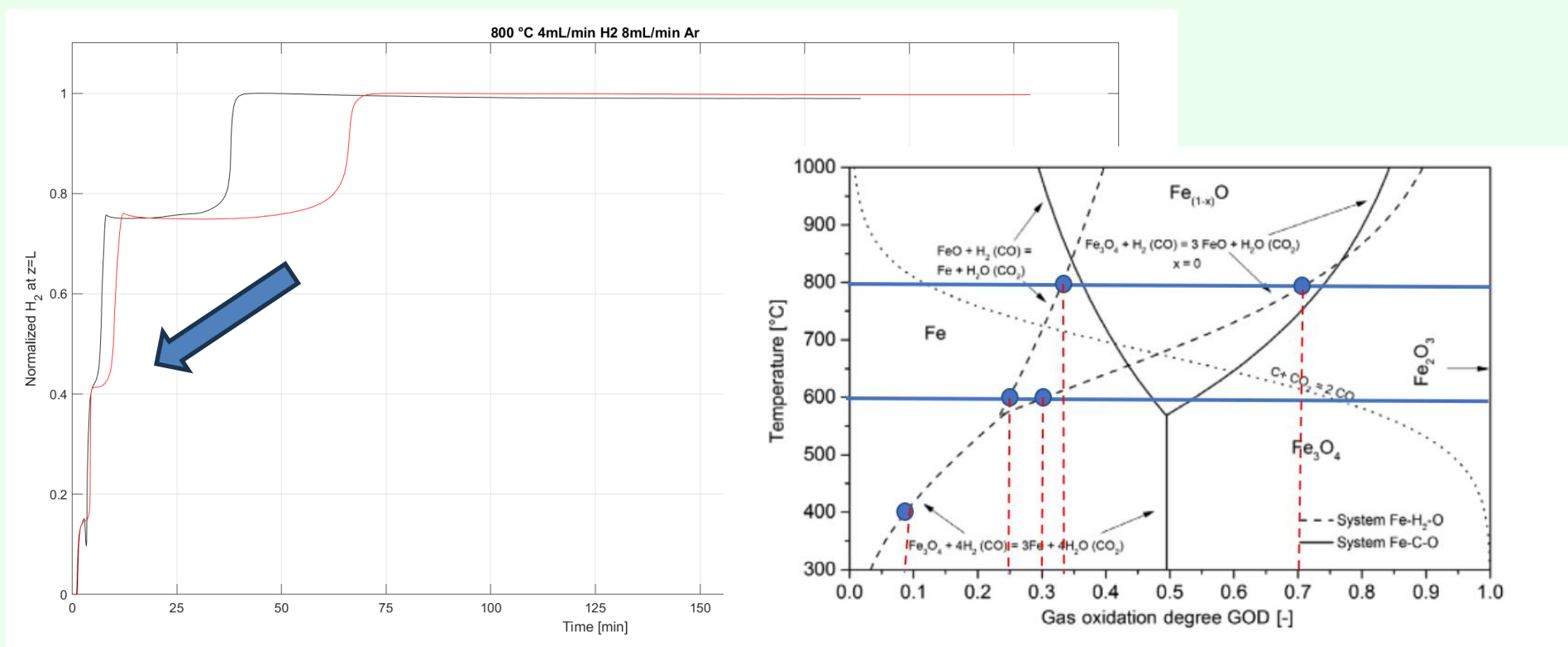
Right panel: 873 K, 11.1 % H₂ (black curve) and 25.0 % H₂ (blue curve). Time to full reduction 65/140 min



Experimental results: Examples (2)

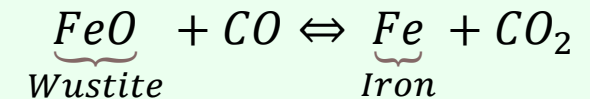
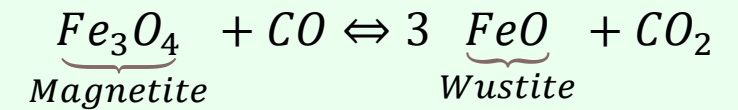
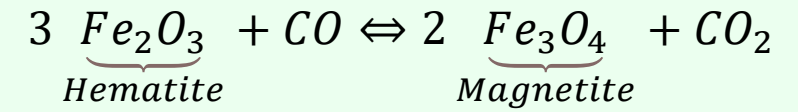
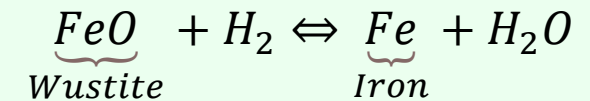
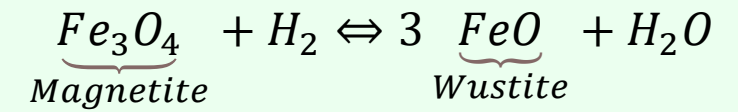
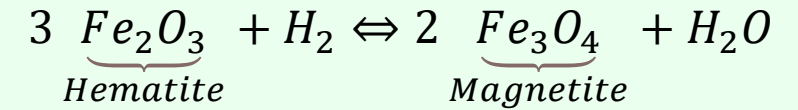
Normalized TCD results of reduction experiments at 1073 K and 33 % H₂ for 100 mg (black curve) and 200 mg (blue curve) bed. As expected, the time to complete reduction practically doubles.

Note the much stronger plateaus (=constant reduction rate) at this higher temperature and hydrogen concentration and the clear appearance of a first plateau!

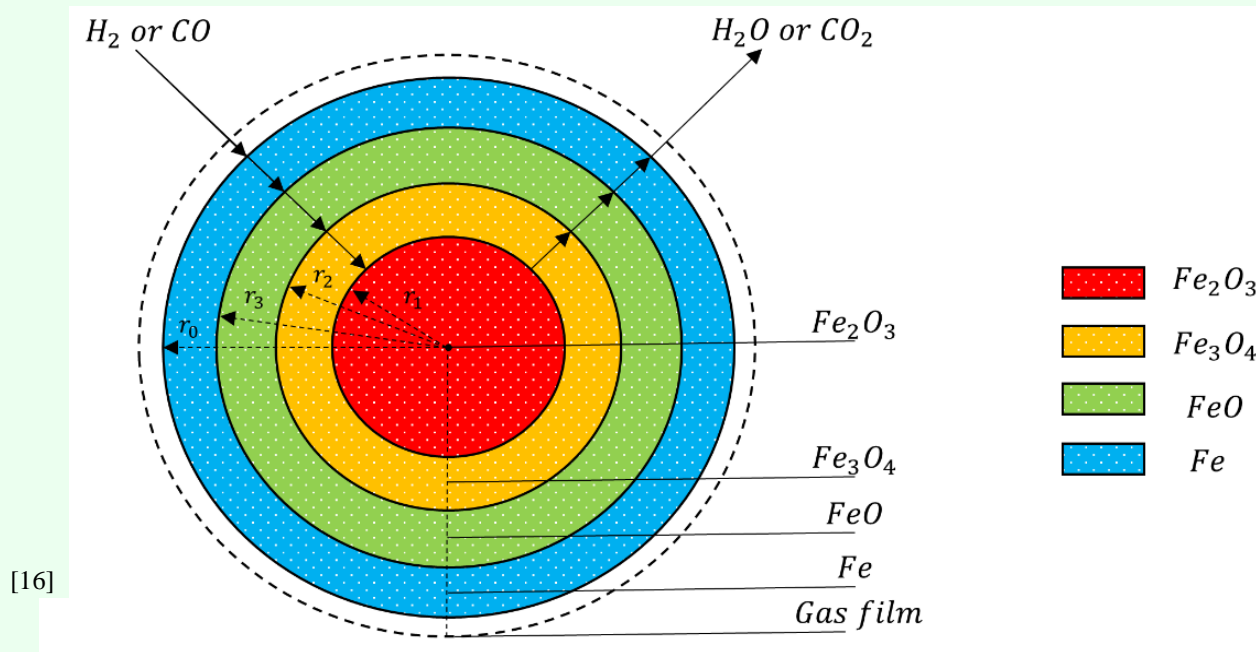


Modelling: Shrinking core approach

Different modeling approaches have been used, Avrami-Erofe'ev model, multi step model or CFD. We apply a three-interface shrinking core model for the three reduction steps from hematite to metallic iron.



Wustite stable for operating temperatures above 843 K



Mathematical model (1)

Starting from the key assumptions of the shrinking core model for the individual particles and the characteristics of the experimental setup with a dynamic particle bed, a mathematical model was developed in MATLAB to simulate the system. Particular attention was paid to the robustness and speed of the model.

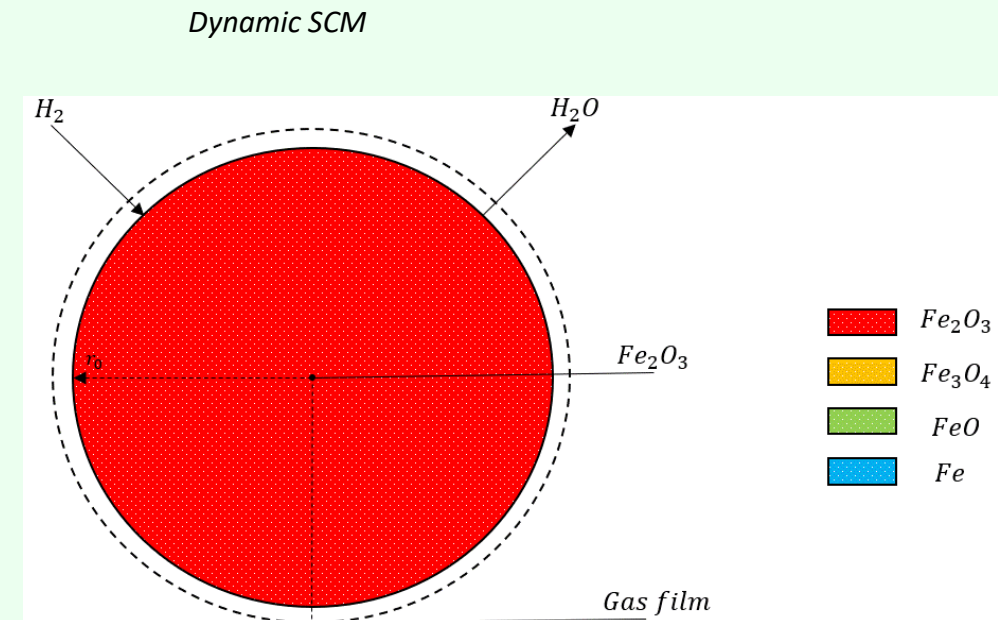
$$\frac{\partial X_j(t, z)}{\partial t} = \frac{r_j(t, z)}{n_0 \cdot a_j}$$

$$\frac{\partial c_i(t, z)}{\partial t} = \underbrace{-\frac{u}{h} \cdot \frac{\partial c_i(t, z)}{\partial z}}_{\text{Convection}} + \underbrace{\frac{D_z}{h^2} \cdot \frac{\partial^2 c_i(t, z)}{\partial z^2}}_{\text{Axial dispersion}} + \underbrace{\frac{1}{(1 - \varepsilon)} \cdot \sum_{j|f}^3 v_{i,j} \cdot r_j(t, z)}_{\text{Reaction SCM}}$$

$$r_j(t, z) = \frac{P}{RT} \frac{3}{r_0} \frac{1}{A_j(t, z)|_f} \cdot \left(\frac{N_j(t, z)|_f}{W(t, z)|_f} - y_{H_2, j, eq}(t, z) \right)$$

Boundary conditions:

$$c_i(t, z) \Big|_{z=0} = c_{i, in} \quad \frac{\partial c_i(t, z)}{\partial z} \Big|_{z=1} = 0$$



Mathematical model (2)

N_j represents the effective reduction contribution of each reaction, while W is the total resistance of the system. Example of hematite ($j=1$) reduction three-front reaction SCM.

$$N_1(t, z) \Big|_3 = (A_1 A_2 A_3) \cdot y_{H_2,1} + [A_1 A_2 (B_3 + F)] \cdot y_{H_2,3,eq} + [A_1 A_3 B_2 + A_1 A_3 (B_3 + F) + A_1 B_2 (B_3 + F)] \cdot y_{H_2,2,eq} \\ + [A_3 B_1 (A_2 + B_2) + A_3 B_1 (A_2 + B_2) + B_1 (A_2 + B_2) (B_3 + F) + A_2 A_3 B_2 + A_2 A_3 (B_3 + F) + A_2 B_2 (B_3 + F)] \cdot y_{H_2,1,eq}$$

$$W(t, z) \Big|_3 = \{ (A_1 + B_1) \cdot [A_3 (A_2 + B_2 + B_3 + F) + (A_2 + B_2) \cdot (B_3 + F)] + A_2 [A_3 (B_2 + B_3 + F) + B_2 (B_3 + F)] \} \cdot y_{H_2,1,eq}$$

$$A_j(t, z) \Big|_f = \frac{1}{(1 - X_j(t, z))^{\frac{2}{3}}} \cdot \frac{1}{k_j \cdot \left(1 + \frac{1}{K_j}\right)}$$

Kinetic resistance

$$B_j(t, z) \Big|_f = \frac{(1 - X_{j+1}(t, z))^{\frac{1}{3}} - (1 - X_j(t, z))^{\frac{1}{3}}}{(1 - X_j(t, z))^{\frac{1}{3}} \cdot (1 - X_{j+1}(t, z))^{\frac{1}{3}}} \cdot \frac{r_0}{D_j}$$

Intraparticle diffusion resistance

$$F = \frac{1}{H}$$

External diffusion resistance

Mathematical model (3)

Dynamic SCM conditions

$$\begin{cases} \text{if } X_1(t, z) < 1 & f = 3 \quad j = 1, 2, 3 \\ \text{if } X_1(t, z) = 1 \cap X_2(t, z) < 1 & f = 2 \quad j = 2, 3 \\ \text{if } X_1(t, z) = 1 \cap X_2(t, z) = 1 \cap X_3(t, z) < 1 & f = 1 \quad j = 3 \end{cases}$$

$$y_{i,j,eq}(t, z) = \frac{1}{(1 + K_j)} \cdot (y_{H_2,j}(t, z) + y_{H_2O,j}(t, z)) \quad \text{Equilibrium composition}$$

$$k_j = k_{j,ref} \exp \left[\left(-\frac{E_{a,j}}{R} \right) \cdot \left(\frac{1}{T} - \frac{1}{T_{ref}} \right) \right] \quad \text{Modified Arrhenius Eq.}$$

$$K_j = e^{\frac{-\Delta G_j}{RT}} = e^{\frac{-(\Delta H_j - T \cdot \Delta S_j)}{RT}} \quad \text{Equilibrium constant}$$

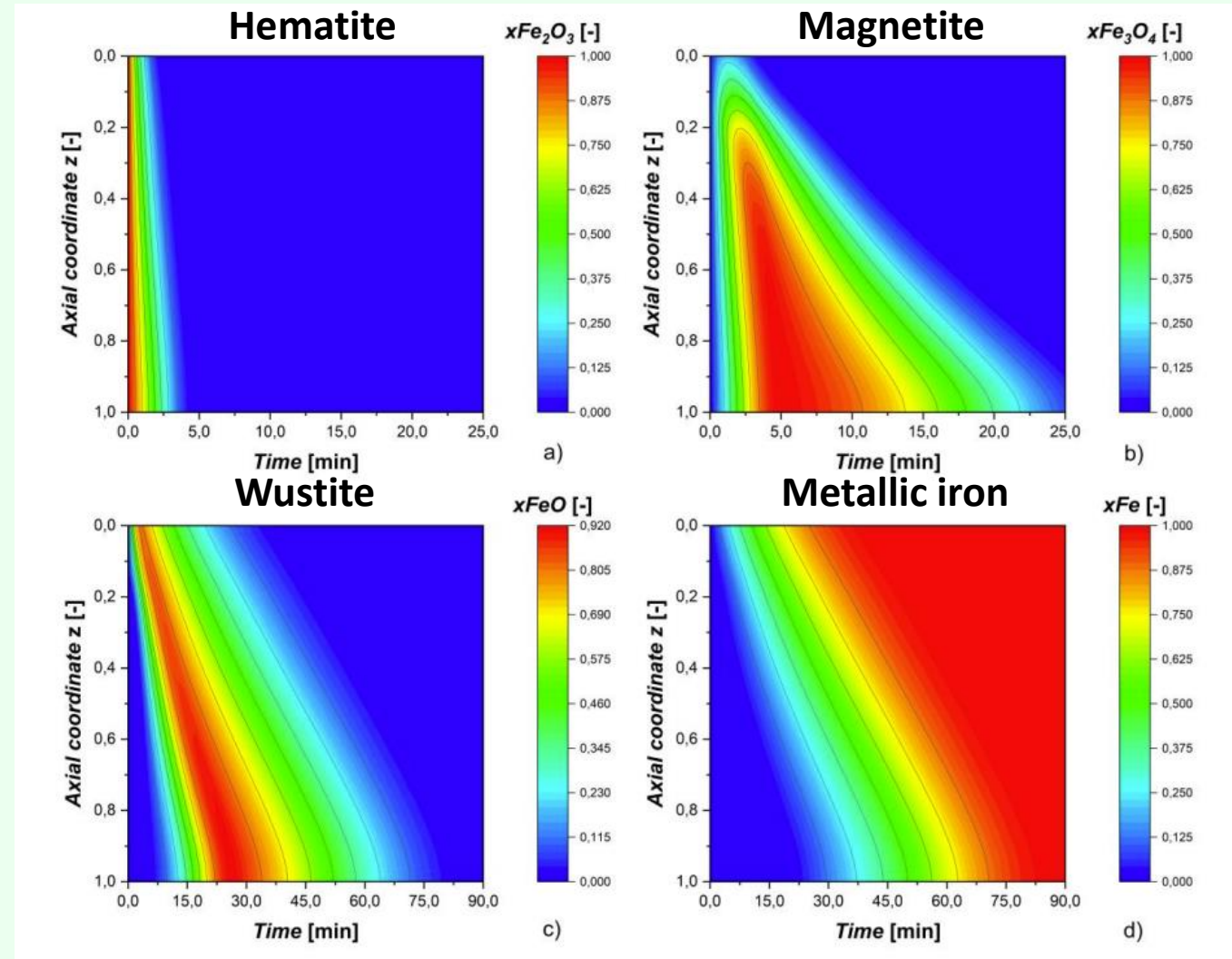
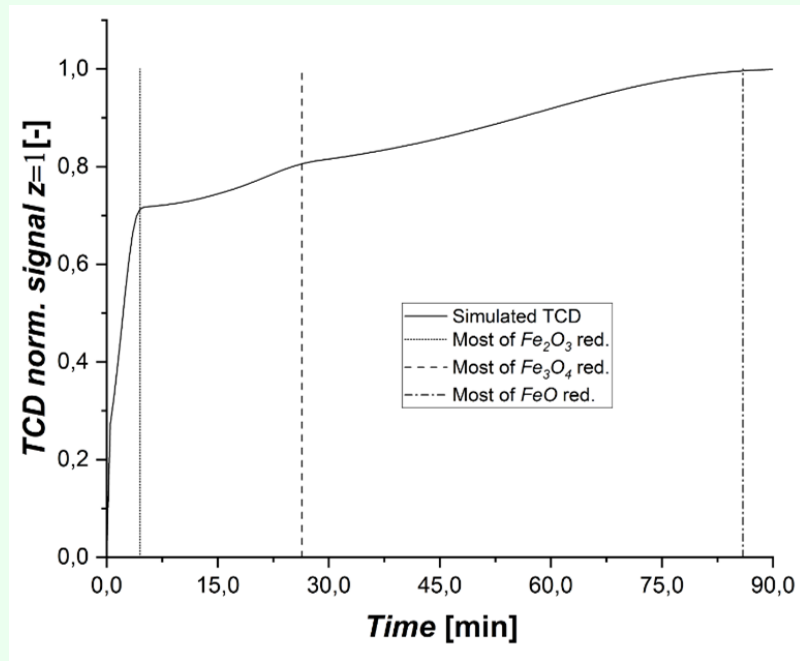
$$D_j = d_{1,j} \cdot e^{d_{2,j} - \frac{d_{3,j}}{T}} \quad \text{Intraparticle diffusion}$$

Parameter	Value	Unit	Parameter	Value	Unit
$d_{1,1}$	$1 \cdot 10^{-4}$	$m^2 s^{-1}$	D_z	$1 \cdot 10^{-6}$	$m^2 s^{-1}$
$d_{2,1}$	3.43	—	$E_{a,1}$	$33.4 \cdot 10^3$	$J mol^{-1}$
$d_{3,1}$	$4.2 \cdot 10^3$	K	$E_{a,2}$	$58.2 \cdot 10^3$	$J mol^{-1}$
$d_{1,2}$	$1 \cdot 10^{-4}$	$m^2 s^{-1}$	$E_{a,3}$	$57.1 \cdot 10^3$	$J mol^{-1}$
$d_{2,2}$	5.64	—	$k_{1,ref}$	$5 \cdot 10^{-5}$	$m s^{-1}$
$d_{3,2}$	$6.8 \cdot 10^3$	K	$k_{2,ref}$	$2 \cdot 10^{-4}$	$m s^{-1}$
$d_{1,3}$	$1 \cdot 10^{-4}$	$m^2 s^{-1}$	$k_{3,ref}$	$4 \cdot 10^{-5}$	$m s^{-1}$
$d_{2,3}$	4.77	—	r_0	$2.5 \cdot 10^{-6}$	m
$d_{3,3}$	$5.9 \cdot 10^3$	K	ε	0.25	—

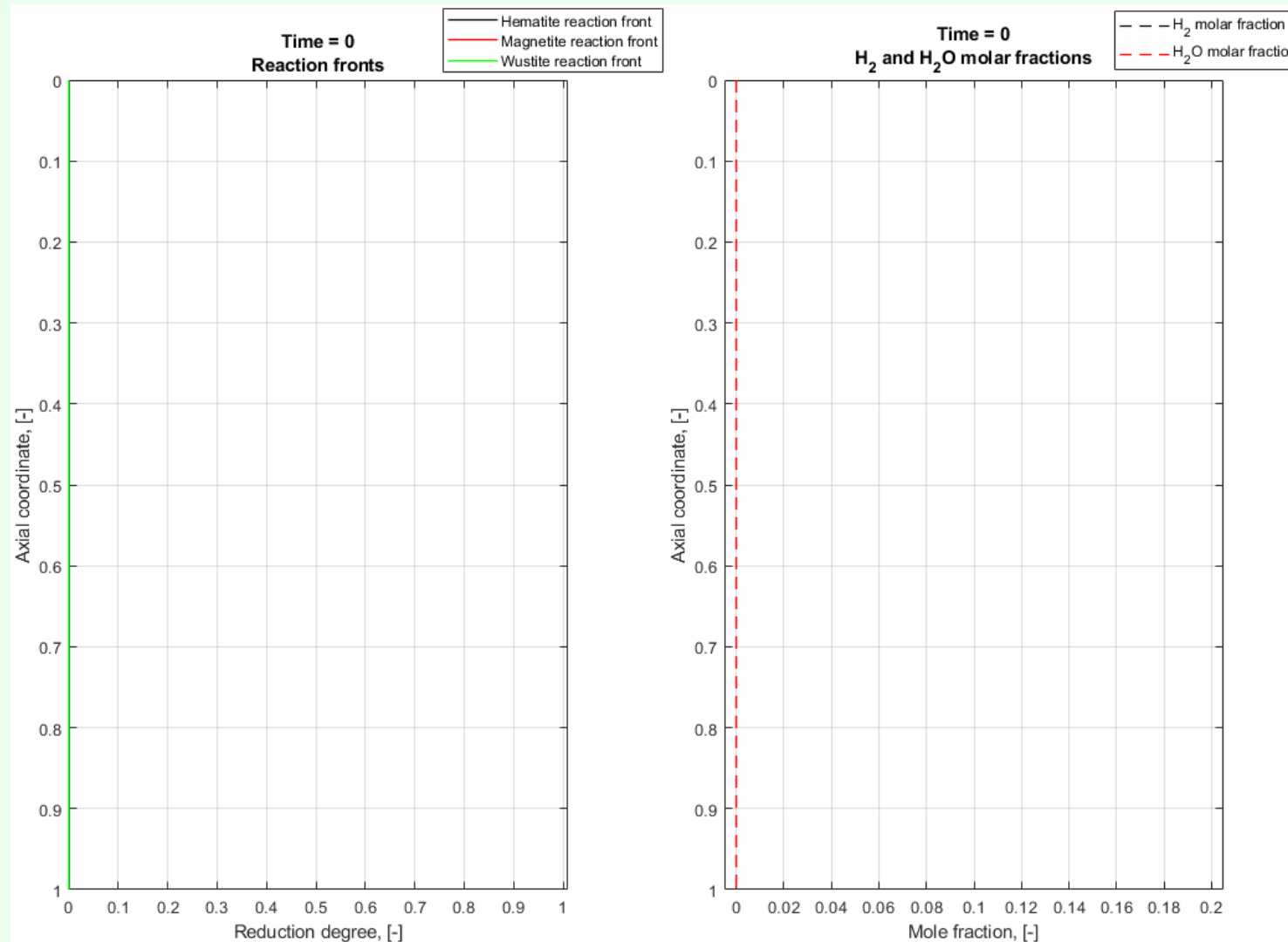
Model simulation

An expression for the thermal conductivity as a function of the gas composition was applied.

Simulating the reduction of 100 mg hematite at 873 K and a gas flow of 20 ml/min, 20 % H₂ yielded the results in the figures.



Evolution of reaction fronts and gas composition



Gas inlet



Gas outlet

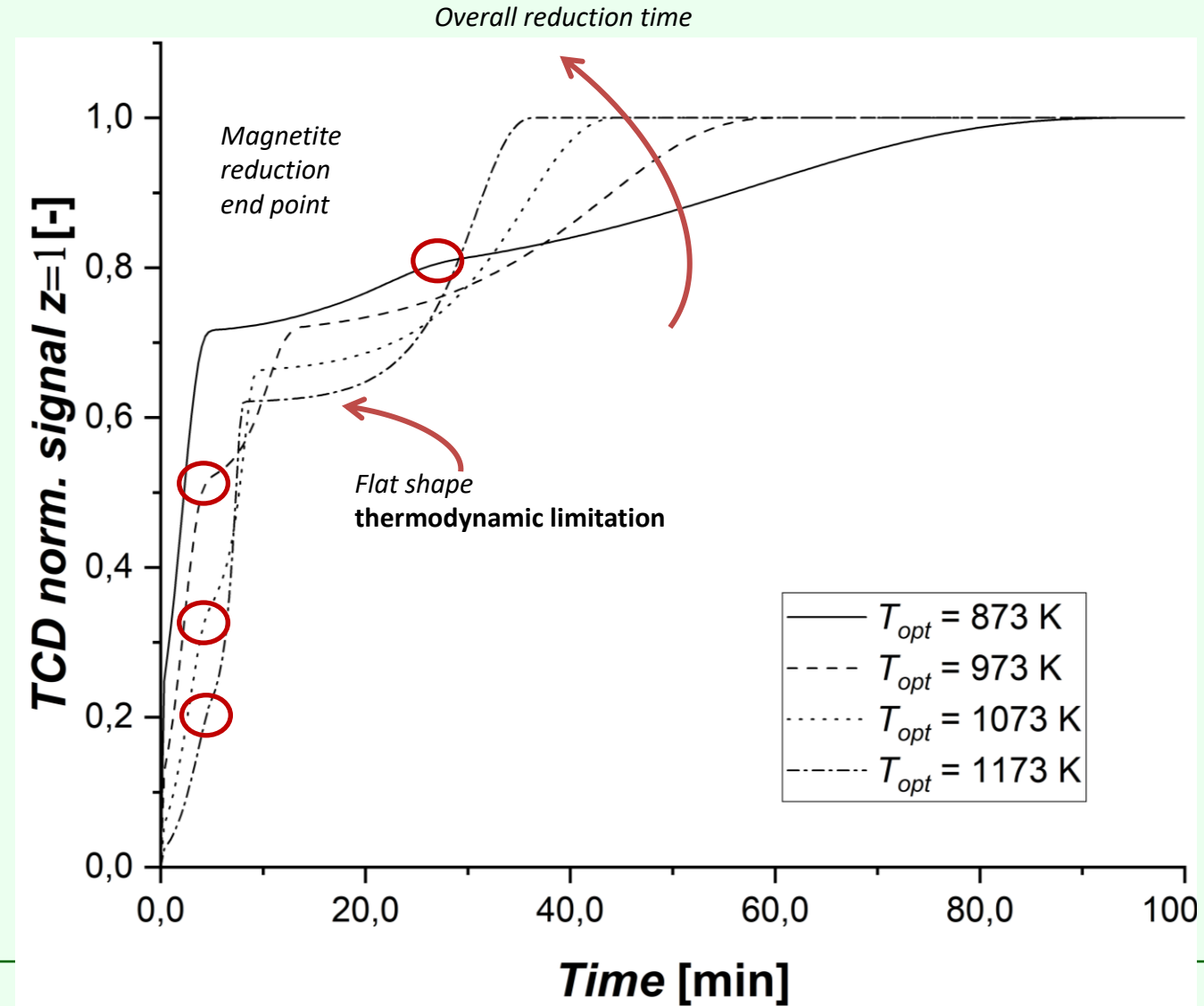
Influence of temperature

Increasing the temperature T shortens the reaction time: at 1173 K the complete reduction time is less than half that of 873 K.

At higher T , the point of complete magnetite reduction becomes less evident due to the sharp change in the slope of the final reactive step.

The simulated signal becomes progressively flatter during the initial stage of the wustite reduction, due to the high presence of H_2O .

The reduction of wustite is strongly thermodynamically limited.

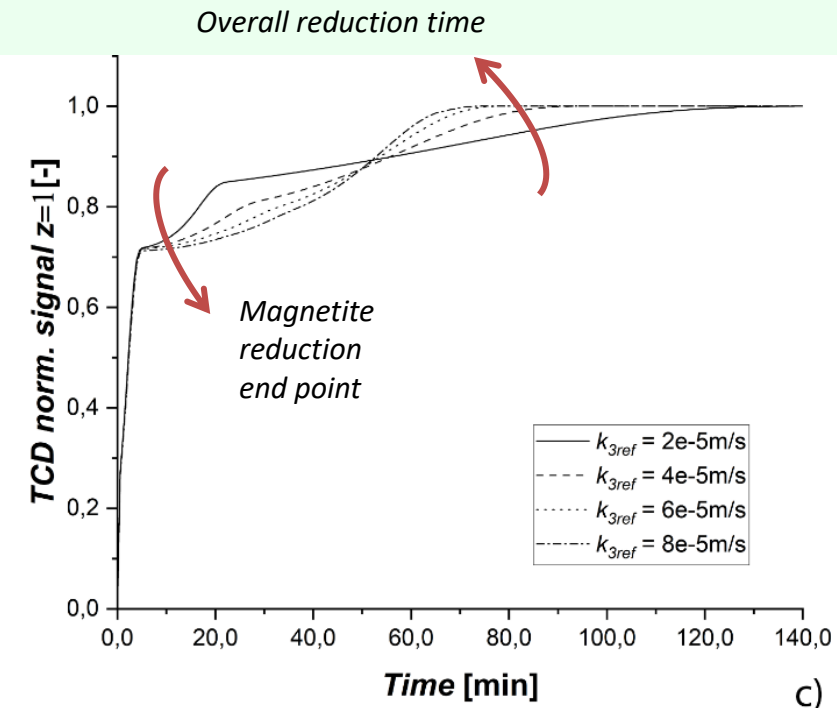
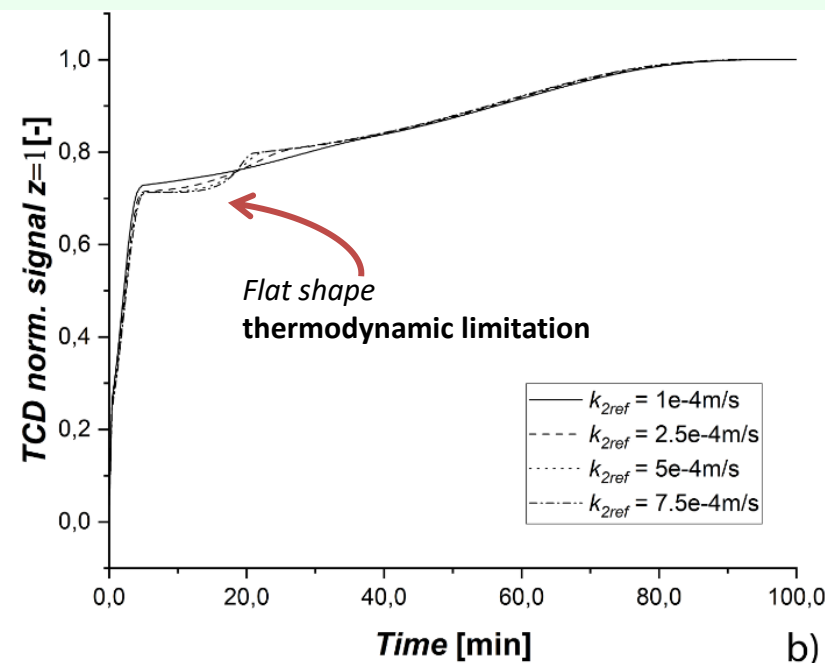
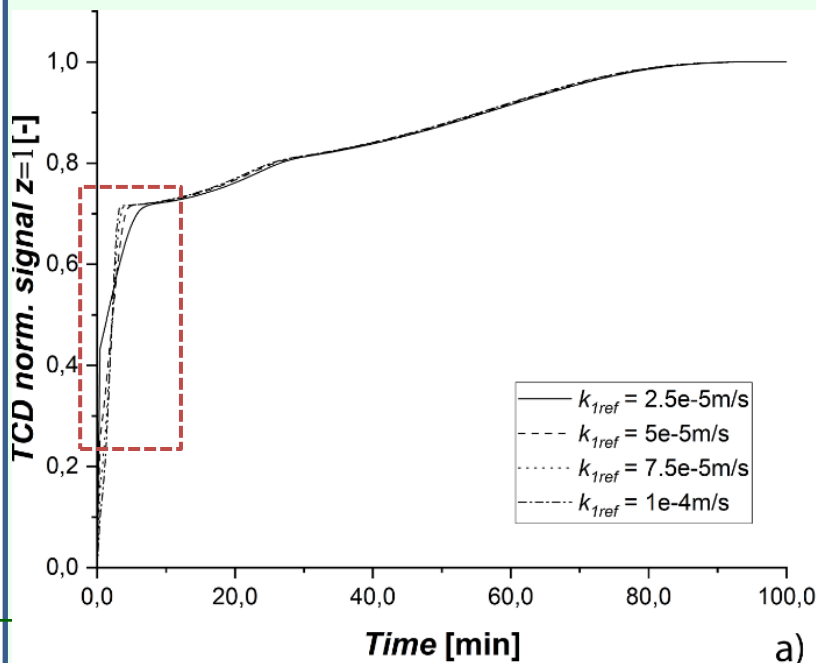


Influence of reference kinetic constants

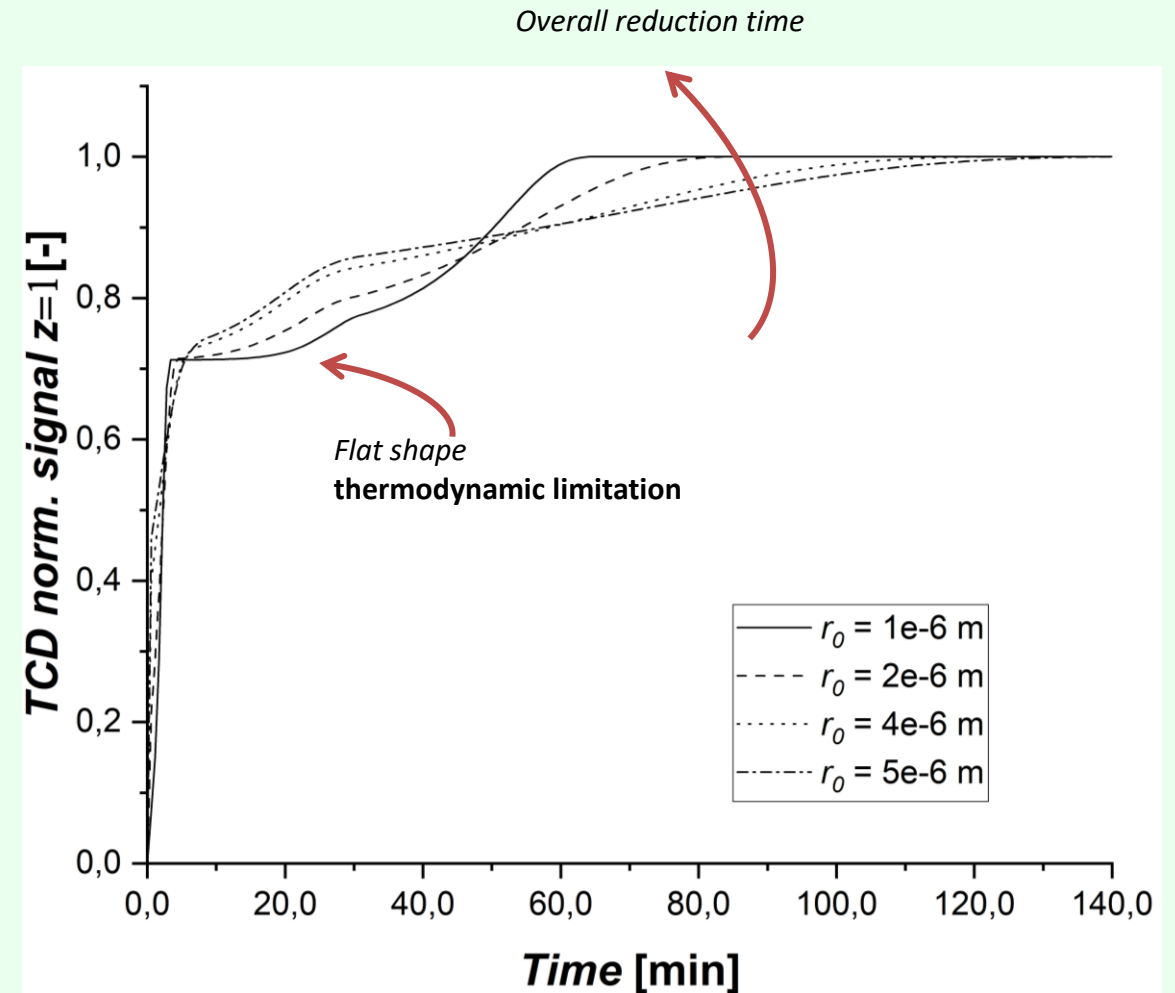
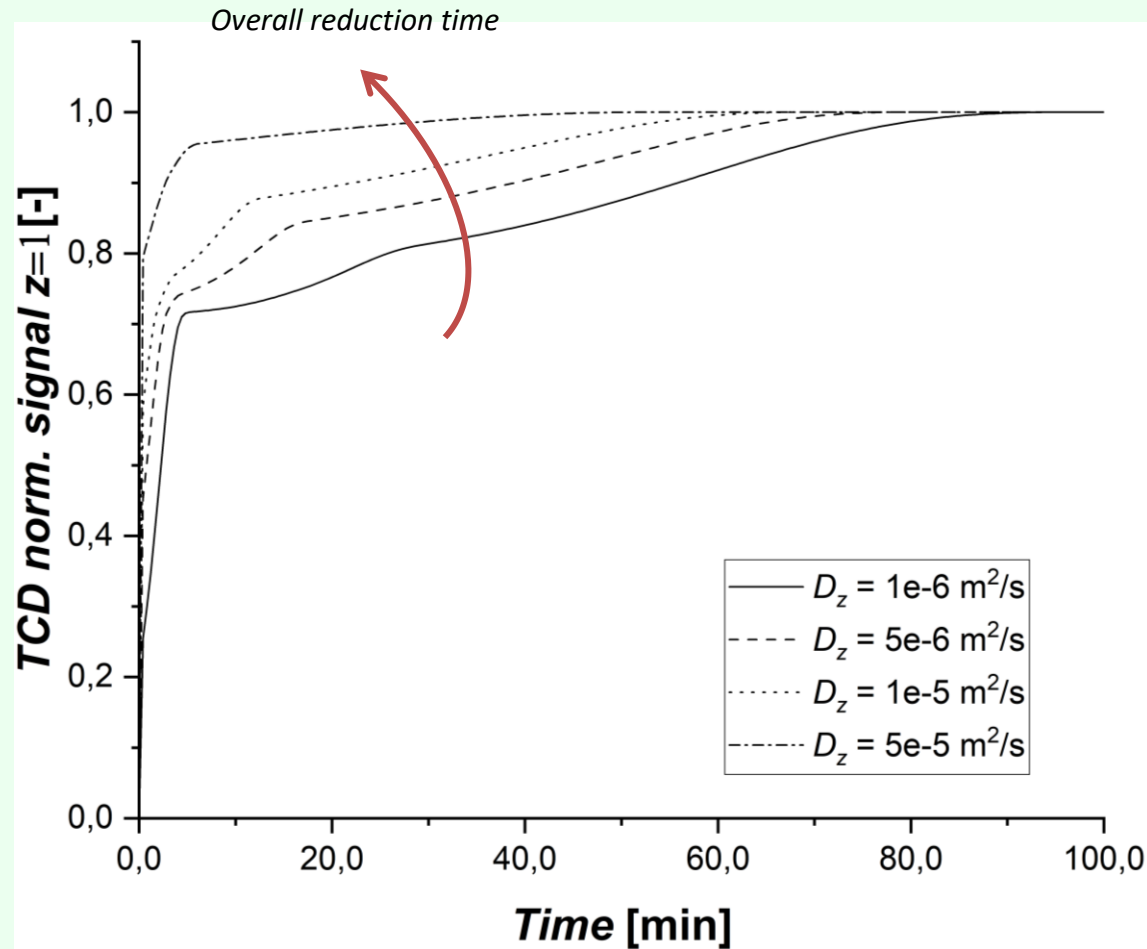
The first pre-exponential constant affects only the reduction of hematite as expected.

The second pre-exponential kinetic constant affects mainly the middle area of the diagram and minimally the part of the signal describing the completion of the hematite reduction.

The third pre-exponential kinetic constant, appears to have the strongest influence on the model results, for both Fe_3O_4 and FeO reduction, being crucial in determining the overall reaction time.

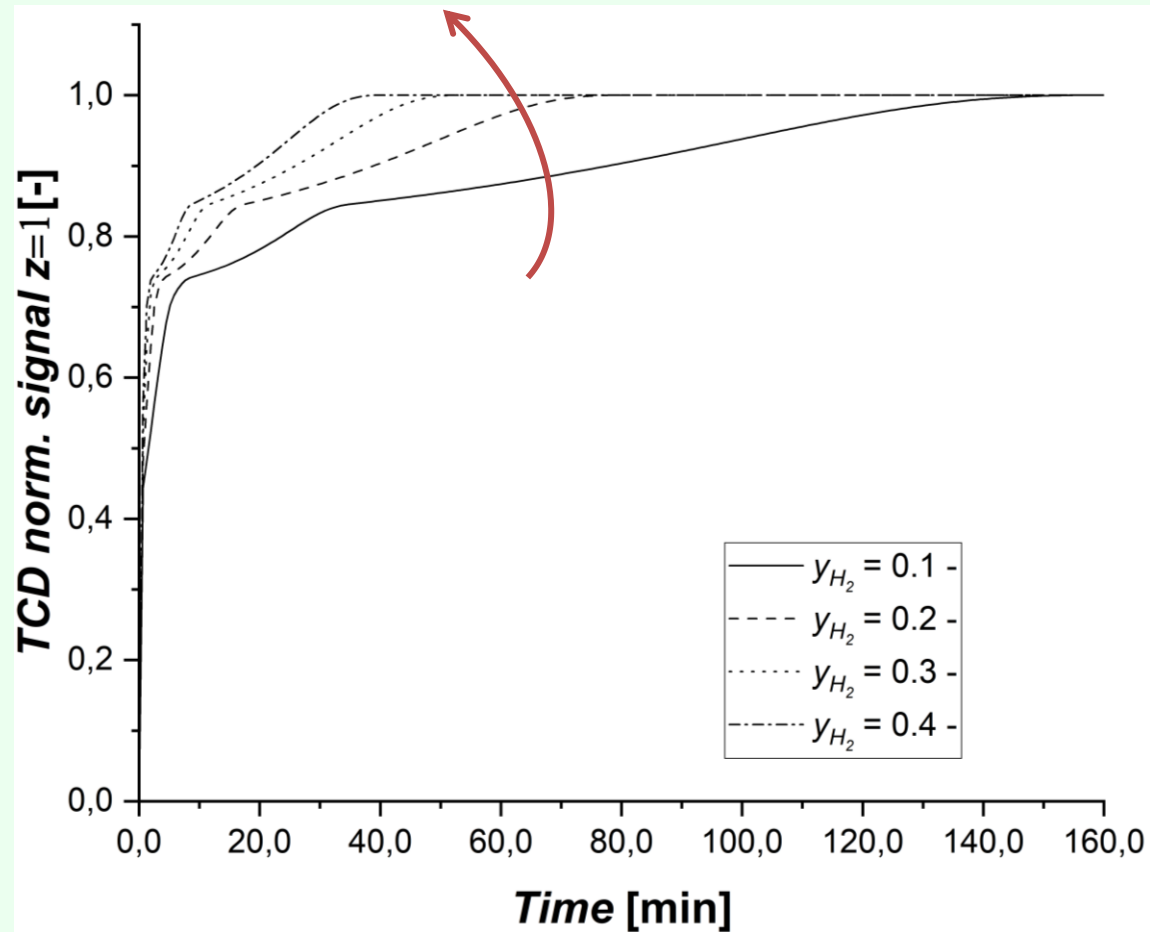


Influence of axial dispersion coefficient and particle radius

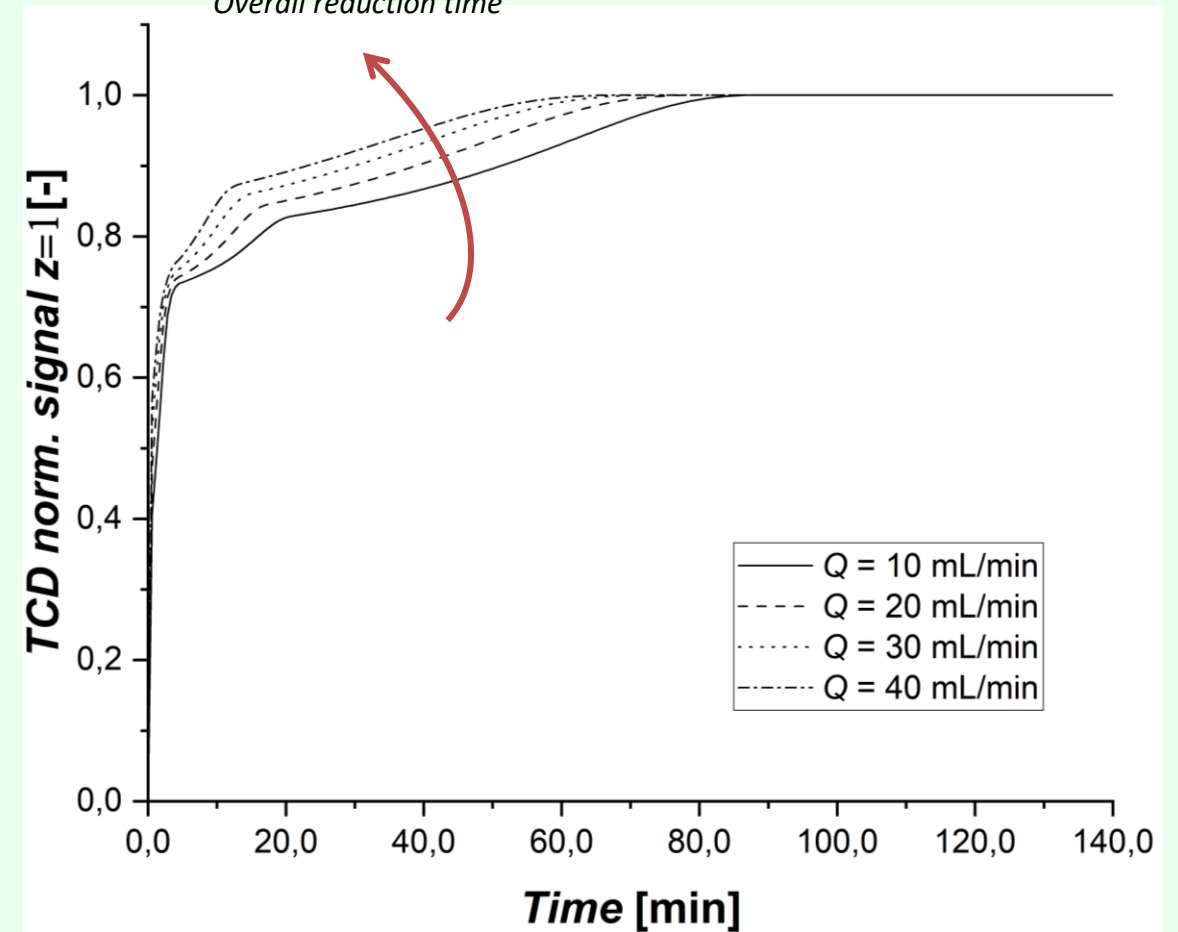


Influence of gas composition and flow rate

Overall reduction time



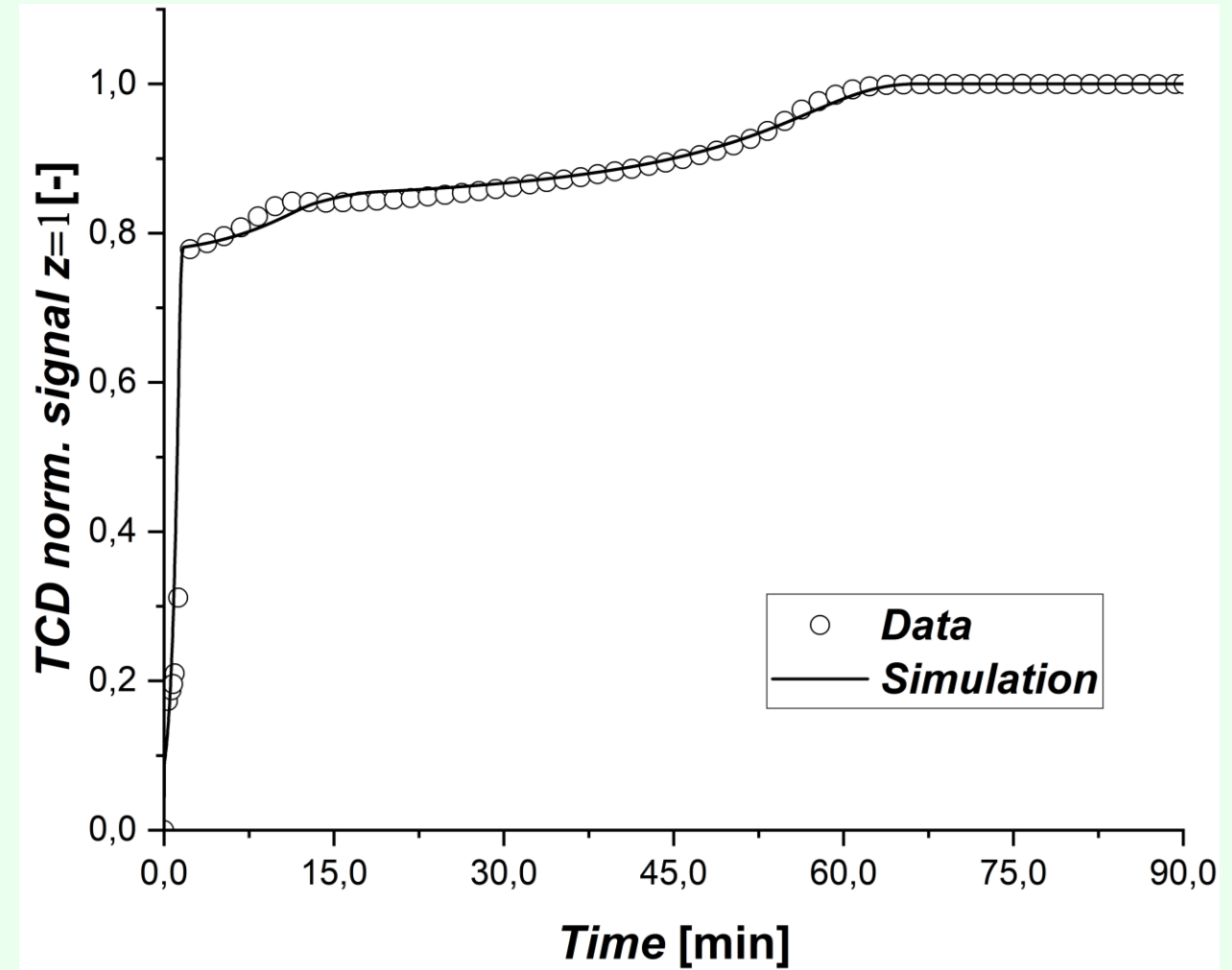
Overall reduction time



Comparison between experimental data and model

After manipulation of the pre-exponential constants and the axial dispersion coefficient for, the model was able to reproduce the TCD signal of a specific experiment.

The model can explain the changes in the slope of the TCD signal as a result of transitions between the reduction steps and the fact that the system may approach equilibrium due to the limited gas flow rate.



Conclusions

Hydrogen reduction experiments in a small bed of iron oxide/ore fines have been undertaken in laboratory scale.

An in-depth modeling study was carried out by applying the main assumptions of the three-interface shrinking core model to a reactive packed bed-like system similar to that of the experiments to describe the reduction processes of iron oxides fines in the presence of H_2

A sensitivity study of the mathematical model was performed by analyzing its responses to parametric perturbation

The model has shown promising predictive ability when compared to data from the reduction experiments.

The acquisition of a large set of accurate experimental data under different operating conditions will allow for the estimation of kinetic parameters of each reaction phase



আপনার মনোযোগের জন্য আপনাকে ধন্যবাদ